Phase structures, loss, storage, damping, voice-absorption, and mechanical properties: NCB/BWZT/RTV

juanjuan wang (juanwang@xaut.edu.cn)
Xi'an University of Technology https://orcid.org/0000-0003-0571-5358
Hua Jiao
Xi'an University of Technology
Qijiu Deng
Xi'an University of Technology
Yaning Feng
Xi'an University of Technology
Yule Yang
Xi'an University of Technology

Research Article

Keywords: Absorption, Damping, Loss, Carbon black, BWZT, Silicone Rubbers

Posted Date: February 12th, 2021

DOI: https://doi.org/10.21203/rs.3.rs-216252/v1

Version of Record: A version of this preprint was published at Journal of Materials Science: Materials in Electronics on August 12th, 2021. See the published version at https://doi.org/10.1007/s10854-021-06769-7.

Abstract

The objective of this work is to characterize the effect of NCB(Nano-carbon black)on the comprehensive performances and micro, chemical and phase structures of NCB/BWZT/RTV composite [BWZT is Ba$(W_{1/2}Cu_{1/2})O_3$-$Pb_{0.98}Sr_{0.02}$ $(Mg_{1/3}Nb_{2/3})_{0.275}(Ni_{1/3}\ Nb_{2/3})_{0.10}(Zr_{0.25}Ti_{0.375})\ O_3$ and, RTV is Room Temperature Vulcanizing silicone rubber.]. Composites with damping-absorption performances and storage-loss behaviors based on RTV, BWZT and, NCB as conductive agent were fabricated employing three steps methods of ball-milling, three-roller milling and pressing. The effects of NCB and its amount on storage, loss and damping properties were investigated by the method of DMTA and, absorption and mechanical performances are measured by the methods of standing wave tube and TG separately. The micro, chemical and phase structures of composites are characterized by SEM, XRD and IR. The results indicated that both doping of NCB and the combination of BWZT and RTV can be proposed to improve greatly the comprehensive performance of RTV matrixes and, there would be more excellent comprehensive properties in NCB/BWZT/RTV composites with amount of 4 wt. %.-6wt. % for NCB as d_{33} of 81 pC/N, *storage modulus* of 25003MPa, *loss modulus* of 398MPa, damping coefficient of 0.07–0.12, and *absorption coefficients* of 0.45–0.55 with the difference of frequency in the range of 400-1600Hz. Also, the lattice growth of BWZT is found showing strong dependences on the contents of NCB and, the absorption and damping performance of composites on frequency and temperature separately.

1 Introduction

Elastomer based on piezoelectrics have become attractive structural and functional noise absorption composites [1–3] in the field of industrial production, aerospace [4], marine, automobile, railways, civil engineering [5], electron, machine and cable industries [11–12], entertainments [6] etc. due to the moderate hardy and elasticity, being easy in perception and processing to environmental signals [7], design abilities in performances [8], combinations in high di-electricity of ceramics and insulativity of polymers [9–10], according with the need of high dielectric, ease to processing and so on. Their high damping-absorption properties own to two sides [13–15]: Viscous damping coming from polymer and piezoelectric damping resulting from piezoelectric. Elastomers will impose mechanical vibration on piezoelectric during its elastic vibration [16], and, the mechanical energy change into electrical ones because of the piezoelectric, which can be dismissed by conductive phase [17]. Moreover, the re-viscous damping can improve own to the cooperation between piezoelectric and elastomers, which leads to the big improvement in damping-absorption properties for conductive phase/ piezoelectric/elastomers [18].

So, generally, the damping-absorption performances and loss of the piezoelectric/ Elastomers composite are defined by the piezo electrical property of piezo electric phase, the elasticity of elastomers, and the cooperation between them, while the conductive phase plays the key role during the process of voice energy exhausted [19–20].

RTV (Room Temperature Vulcanized Silicon Rubber) is the most commonly used elastomer matrix for noise absorption applications own to its high elasticity and damping performances. BWZT [Ba $(W_{1/2}Cu_{1/2})O_3$-$Pb_{0.98}Sr_{0.02}$ $(Mg_{1/3}Nb_{2/3})_{0.275}(Ni_{1/3}Nb_{2/3})_{0.10}$ $(Zr_{0.25}Ti_{0.375})$ O_3] is used as piezoelectric for its high piezoelectric property, and, NCB (Nano-Carbon Black), NG (nano-graphite) and CNT (Carbon Nano-tube) etc. as conductive phase for their high conductive features.

To improvement the comprehensive properties of Piezoelectric/Elastomers, composites with damping-sound absorption performances based RTV as elastomer matrix, BWZT as piezo-electrical modifier, and, NCB as conductive phase were fabricated employing three steps of ball-milling, three-roller milling and pressing methods.

The primary interest of this paper was to characterize the effect of NCB on the micro, chemical and phase structures of NCB/BWZT/RTV composites. Standing wave tube methods were used to evaluate absorptions. Thermo-gravimetric analysis (TGA) and dynamic mechanical analysis (DMTA) were performed to evaluate the thermal, storage, loss modules and damping performances.

2 Experimental

2.1 Raw materials and materials

The RTV matrixes with a brand name of number 107 Rubber were purchased from Chenguang Chemical Institute, Zigong city of Sichuan, China. And, Methyltris (methylethylketoxime) silicone (D-30) as a cross-linking agent, dibutyl tin laurate (D-80) as a catalyst, KH550 as a coupling agent, were provided by Xiantao Chemical Co., Xiantao city of Wuhan, China. The raw materials PSZT was purchased from Beijing Safe Lab Technology Co. Ltd and Xi'an Konghong Information Technology Co., Ltd separately, Xi'an, China. BWZT was obtained from PSZT [$Pb_{0.98}Sr_{0.02}$ $(Mg_{1/3}Nb_{2/3})_{0.275}(Ni_{1/3}Nb_{2/3})_{0.10}(Zr_{0.25}Ti_{0.375})$ O_3] and BWC [Ba $(W_{1/2}$ $Cu_{1/2})$ O_3] by using the method of solid sintering. Pb_3O_4, $SrCO_3$, $MgCO_3$, Nb_2O_5, NiO, ZrO_2, TiO_2, $BaCO_3$, WO_3 and CuO were bought from raw material market with purity of 99.99%. NCB was bought from XFNANO Materials Tech Co. Ltd, Nanjing, China. Besides all of these, there were 102□gasoline as solvent, which were obtained from common market, China.

2.2 Preparation of NCB/BWZT/RTV composites

RTV matrix were prepared with process of reactive solution mixing, and, stored as reacted mixtures hermetically to avoid curing in the air.

The raw materials such as NCB and BWZT power were mixed by wet ball milling on the condition of 350r/min 6-8h according to rations of Table 1 after 95 ^oC /2-4h dryer. The solvent was evaporated away after ejection of compact. And then, the dry powder was mixed with RTV pre-polymer mixtures away of most of solvent for 1-2hs by the process of three-roller milling. The final mixtures were pressed into wafer in the diameter of 10cm with the self-made mold on the common powder sheeting-out mill. The wafer

were polarized for 15min with high voltage of 8-10kV in silicone oil on the condition of no over breaking after multi-meter checking, and electrode overlaying with Ag-Pd. The final composite is OK.

2.3 Characterizations

The morphology of the fracture surface of the composite was examined using a scanning electron microscope (SEM) (SEM, HITACHI-570). XRD was used to inspect the phase structure and crystalline state of composite. The chemical structure was demonstrated by IR (Fourier transform Infrared Spectrometer, EQUINX55).

2.4 Property tests

The piezo electrical performance of NCB/BWZT/RTV composites was measured by a quasistatic piezoelectric meter (ZJ-3d, Institute of Acoustics Academic were sinica, Beijing, China). For temperature-dependent polarization-electric field (P-E) hysteresis and strain measurement, the top electrode was connected to a high voltage amplifier (Model 610E, Trek, USA) for the electrical loading. DMTA were used to demonstrate the damping performance, the loss and storage modulus. The absorption coefficient was measured by standing wave tube. In the end, heat-resistant property of composites was inspected by TG (TG, Q600SDT).

3 Results And Discussion

3.1 Morphologies of damping-absorption composites

Fig.1 presented the microstructures of NCB/BWZT/RTV composites with different NCB amount. It could be found that the addition of NCB didn't have much impact on the micro structure of BWZT/RTV matrix. There was good compatibility between BWZT and RTV with the NCB amount of 0 wt. %. The fracture surface of composites showed the spots whose densities improved with the increase of NCB content, which demonstrated a more rough section, and, a transition to ductile fracture. The accumulation happened at the fracture of NCB 6wt. %/BWZT/RTV. So, it can be found that composite 4wt. %/BWZT/RTV was of the best morphologies.

3.2 Infrared spectrum

Fig.2 was the infrared spectrums of RTV, BWZT/RTV, 1wt. %NCB/ BWZT/RTV and 6wt.%NCB/BWZT/RTV composites. The peak in 732cm^{-1}and 789cm^{-1} indicated the absorption of -Si-O-Si- in RTV（720cm^{-1}-840cm^{-1}）, and, peaks in 1032cm^{-1} and 1102cm^{-1} indicated the absorption of in -Si（CH_3）$_2$-. The peak in 1510cm^{-1} and 1626cm^{-1} shows physical absorption of OH^- in water（1500cm^{-1}-1650cm^{-1}）, while peaks in 3543cm^{-1}, 3657cm^{-1} and 3751cm^{-1} demonstrated the all absorption of OH^- in water coming from physical and chemical absorptions（3200cm^{-1}-3750cm^{-1}）. The peaks show above couldn't sharpen or blunt, which showed that the additions neither BWZT nor NCB affected the structures of RTV.

So, it can be concluded from Fig.2 that the additions of BWZT or NCB couldn't lead to the changes and crosslinking in chemical **structure of RTV, and, the** interface bonding of BWZT/RTV complex matrix and NCB/PZT/RTV composites is physical ones.

3.3 XRD of composites

Fig.3 shows the XRD of RTV、BWZT/RTV and NCB/BWZT/RTV composites with different NCB amounts (with the NCB content of 1 wt.%, 4 wt.% and 8 wt.%). Firstly, the peak can be found for series of composites with different NCB amounts, but not for RTV and BWZT/RTV, which shows the addition of NCB can impose crystallization on BWZT.

Secondly, it can be found from Fig.3 that both of BWZT/RTV complex matrix and NCB/BWZT/RTV composites with different NCB amounts present **single perovskite in structure**, and, neither **pyrochlore phase** nor the second phaseis found. The 〖002〗$_R$ phase at $2\theta=45^{\circ}$ demonstrates the single rhombohedral phase of composites. And, there is no splitting in the peaks for neither composites with different NCB amounts nor BWZT/RTV complex matrix when $2\theta=45^{\circ}$, which demonstrates both them has not turn into tetragonal phase and will not. Differently, both main and secondary peaks of composites with different NCB amounts moves left lightly compare with BWZT/RTV complex matrix, and, it will be more with the improvement of NCB amounts.

So, it can be concluded that the improvement in NCB amounts for composites can lead to the growth in all lattice parameters of BWZT, but, it did not cause the preferential growth in any a single crystal surface.

3.4 Piezoelectric property of composites

The piezoelectric property before and after high voltage poling of NCB/BWZT/RTV composites with NCB amount from 0wt.% to 8wt. % is presented in Table 2. It can be found that the value of d_{33} increase from 58 pC/N before poling to 66 pC/N after poling for composites with NCB amount of 0wt.%, which demonstrated that the secondary poling with high voltage can advance the improvement in piezoelectric property for BWZT/RTV complex matrix. It can be concluded the improvement in piezoelectric property originates from the re-poling of dipoles which did not be poled well firstly because of difficulties in this.

Secondly, BWZT/RTV complex matrix shows a much lower piezoelectric property than BWZT (The original d_{33} of BWZT was 546pC/N, while which of BWZT/RTV is in 58-81 pC/N as what was listed in the Table 2.), which means doping with RTV can decrease the piezoelectric property of BWZT because of the damping and vibration extinction effect of RTV. And, the 6wt.%NCB/BWZT/RTV is of the highest value of 81 pC/N in d_{33} after the secondary poling with high voltage.

Thirdly, it is presented that the piezoelectric property improved both before and after poling with the the increasing of NCB amount, which demonstrated that NCB can induce to a higher piezoelectric property for BWZT/RTV complex matrix. So, it can be concluded that it is necessary to polorize the BWZT/RTV

complex matrix at the second time with a higher voltage, while the conductive phase NCBcan imposed induction effect on the piezoelectric performance of BWZT/RTV.

3.5 Loss of composites

Ferroelectric hysteresis loops of BWZT/RTV and NCB/BWZT/RTV composites with different NCB amounts are showed in the Fig.4. NCB 1wt. %/BWZT/RTV-NCB 8wt. %/BWZT/RTV etc. is typified by NCB1/BWZT/RTV-NCB8/BWZT/RTV and so on in the graphs respectively and, the same after this. From the area difference in Fig.4, it can be concluded that the addition of NCB and its contents lead a different effect on internal loss of BWZT/RTV complex matrix. And, the internal loss follows the order of NCB6/BWZT/RTV, NCB8/BWZT/RTV, NCB4/BWZT/RTV, NCB2/BWZT/RTV, NCB1/BWZT/RTV, and BWZT/RTV from the biggest to the smallest. It can be found that the internal loss of BWZT/RTV improves with addition of NCB, and, it increase with the improvements in contents of NCB when lower than 6wt.% , while there are opposite tendency with contents of NCB when higher than 6wt.%. It's thought that it is the decreasing in flexibility of deflections and the increasing in friction each other and mutual interference for domain with the addition of NCB that imposed the more loss on NCB/BWZT/RTV composites with the improvements in contents of NCB when lower than 6wt.%, while parts of dipoles do not deflect at all because of crowd coming from improvement in NCB contents. On the other hand, there will be no frictional loss when dipoles can’t contact each other because of more internal defects coming from the increasing of NCB doping, which lead to the decreasing in the whole internal loss of composites.

3.6 DMTA of composites

Fig.5 is the storage modulus of BWZT/RTV complex matrix and NCB/BWZT/RTV composites with different NCB amounts. It can be found from Fig.5 that doping with NCB can advance the storage modulus of BWZT/RTV complex matrix, but the improvements are different with the difference in the contents of NCB. On the other hand, temperature is the key point for the storage modulus both BWZT/RTV complex matrix and NCB/BWZT/RTV composites with different NCB amount. The improvements of BWZT/RTV complex matrix and NCB/BWZT/RTV composites with different NCB amount follow the order of NCB8/BWZT/RTV, NCB6/BWZT/RTV, NCB4/BWZT/RTV, NCB2/BWZT/RTV, NCB1/BWZT/RTV, BWZT/RTV from the biggest to the smallest at the temperature of -25 ^{o}C to 175 ^{o}C, which shows that the storage modulus improve with the increasing in contents of NCB. So, it can be concluded that the high contents of NCB will beneficial to the advancement of the storage modulus on the content of 0-8wt.% for NCB when the temperature is lower than 175 ^{o}C. While the improvements of BWZT/RTV complex matrix and NCB/BWZT/RTV composites with different NCB amount follow the order of NCB6/BWZT/RTV, NCB8/BWZT/RTV, NCB4/BWZT/RTV, NCB2/BWZT/RTV, NCB1/BWZT/RTV, BWZT/RTV from the biggest to the smallest when temperature above 175 ^{o}C, which demonstrate that the storage modulus increases first and then decreases with the increase of NCB content. And, the storage modulus of NCB8/BWZT/RTV can get to 31000 MPa, it is 6.32 times higher than 4900 MPa of BWZT/RTV complex matrix. More practical is that the storage modulus of NCB8/BWZT/RTV gets to 26500MPa at the temperature of 25 ^{o}C, it is 4.41 times higher than 4900 MPa of BWZT/RTV complex

matrix. While that of NCB6/BWZT/RTV is 25003MPa, it is 4.10 times higher than 4900 MPa of BWZT/RTV complex matrix. **These suggest that the doping with** NCB can impose great improvement on the storage modulus of BWZT/RTV complex matrix, while there are inconsistent Influence for it, and temperature are **the most inside factors.**

Fig. 6 represents the loss modulus of BWZT/RTV complex matrix and NCB/BWZT/RTV composites with different NCB amounts. It can be observed clearly from Fig. 6 that the doping with NCB can improve the loss modulus of BWZT/RTV complex matrix, and the improvement vary with the difference of CNB content. The loss modulus vary from the biggest to the smallest in the order of NCB6/BWZT/RTV, NCB8/BWZT/RTV, NCB4/BWZT/RTV, NCB2/BWZT/RTV, NCB1/BWZT/RTV, BWZT/RTV for BWZT/RTV complex matrix and composites besides of which the loss modulus of NCB6/BWZT/RTV and NCB8/BWZT/RTV, NCB4/BWZT/RTV, NCB2/BWZT/RTV, NCB2/BWZT/RTV and BWZT/RTV matrix is almost equal respectively. The loss modulus of NCB6/BWZT/RTV maximums to 380MPa, it is increased by 1.9 times than the 200MPa of BWZT/RTV based system. And, **what is further helpful is** 398MPa of NCB6/BWZT/RTV; it is improved 35.4% than the 294MPa of BWZT/RTV matrix at the temperature of 25 ^{o}C. So, the studies above indicate that NCB6/BWZT/RTV will be the ideal loss composite material for sound absorption and noise reduction.

The dynamic mechanical properties of BWZT/RTV complex matrix and NCB/BWZT/RTV composites with different NCB amounts are demonstrated in the Fig.7. It is demonstrated that doping with the NCB can improve the damping performance of BWZT/RTV complex matrix slightly, and temperature is another key point about it. The whole tendency is that the damping performance shows a little increasing with the increasing of temperature, and, the damping coefficients of BWZT/RTV, NCB1/BWZT/RTV, NCB2/BWZT/RTV, NCB4/BWZT/RTV, NCB6/BWZT/RTV and NCB8/BWZT/RTV locate in the range of 0.02-0.05, 0.02-0.15, 0.02-0.75, 0.05-0.4, 0.07-0.12 and 0.03-0.12 respectively. The more **practical datum is that the** damping coefficients of NCB6/BWZT/RTV and NCB8/BWZT/RTV are equal almost at the 25 ^{o}C ($\tan\delta = 0.05$) . Finally, one can see clearly that NCB/BWZT/RTV composite with different NCB amounts has a wider effective temperature range and, the damping coefficient in the range of 0.02-0.4. So, all the NCB/BWZT/RTV composite will be the ideal damping material for absorption with the NCB amount from 1wt. % -8wt. %.

3.7 Absorption of composites

The sound absorption performances with different frequency of BWZT/RTV based system and NCB/BWZT/RTV composite with different NCB amounts are showed in Fig.8. It can be observed clearly from Fig.8 that doping with NCB can promote the sound absorption performance of BWZT/RTV complex matrix, but, the increasing scale differ with the percent of NCB. The sound absorption coefficients of NCB/BWZT/RTV composites are BWZT/RTV of 0.1-0.2, NCB1/BWZT/RTV of 0.18-0.28, NCB2/BWZT/RTV of 0.2-0.34, NCB4/BWZT/RTV of 0.26-0.36, NCB6/BWZT/RTV of 0.45-0.55 and NCB8/BWZT/RTV of 0.5-0.6 respectively, among of these the absorption coefficient of NCB6/BWZT/RTV decreases when frequency overtop 1400Hz. So, it can be concluded that the absorption coefficients of series of

NCB/BWZT/RTV composites increase from 0.1 of BWZT/RTV to 0.55 of NCB6/BWZT/RTV and NCB8/BWZT/RTV on the condition of NCB contents of 0-8wt. % with an increasing rate of 450%. Lastly, it can be found that the absorption property of both BWZT/RTV matrix and NCB/BWZT/RTV composites doesn't vary with the difference of frequency in the range of 400-1600Hz except for NCB6/BWZT/RTV composite.

3.8 TGA of composites

Fig. 9 shows TGA curves of BWZT/RTV complex matrix and NCB/BWZT/RTV composites with different NCB amounts. We can find that the addition of NCB can improve both the pre-decomposition and ending decomposition temperature of BWZT/RTV complex matrix on the condition of NCB amounts from 1wt.% - 8wt.%, while it doesn't affect the thermal decomposition mechanism of BWZT/RTV matrix for the shape of TGA curves for both BWZT/RTV matrix and NCB/BWZT/RTV composites being not changed except for just a moving to right. It is observed that the heat resistant performance of NCB8/BWZT/RTV, NCB6/BWZT/RTV and NCB4/BWZT/RTV are almost equivalent but better than BWZT/RTV complex matrix when the temperature is lower than 500 ^{o}C. And, the three samples are of the higher residual mass than BWZT/RTV matrix at 500 -900 ^{o}C. So, it can be concluded that the addition of NCB can advance the heat resistance of BWZT/RTV matrix, while the contents play a weak role with the range of NCB4 wt. %.-8wt. %.

4 Conclusions

The paper concludes that RTV matrix can be endowed an excellent mechanical, damping, and absorption properties by combining with lead-free based systems of BWZT, and, doping with NCB as conductive phase even. The composites NCB/BWZT/RTV with the ration on weight of 2:3 for BWZT to RTV and amount of 4 wt. %.-6wt. % for NCB demonstrated outstanding comprehensive properties: d_{33} = 81 pC/N, *storage modulus* = 25003MPa, *loss modulus* = 398MPa, *damping coefficient tanδ* of 0.07–0.12, and *absorption coefficients* of 0.45–0.55 with the difference of frequency in the range of 400-1600Hz. Moreover, the improvement in NCB amounts for composites can lead to the growth in all lattice parameters of BWZT, but, it did not cause the preferential growth in any a single crystal surface.

Declarations

Acknowledgement

This work was supported by National Natural Science Foundation of China (No. 51707153), the Shaanxi Province Key Laboratory of Science and Technology Innovation Project (2014SZS09-K04, 2014SZS09-Z01), the Natural Science, and Special fund of Education Department Foundation of Shaanxi Province of China (101-221206, 101-431116033) and Science Foundation of Xi'an University of Technology in China (2015TS002, 101-2560816012).

References

1. M.F.H Wolff, V. Salikov, S. Antonyuk, S. Heinrich, G.A. Schneider, Novel, highly-filled ceramic-polymer composites synthesized by a spouted bed spray granulation process, Compos. Sci. Technol. 90, 154-159 (2014).
2. S. Besset, M.N. Ichchou, Acoustic absorption material optimization in the mid-high frequency range, Appl. Acoust. 72, 632-638 (2019).
3. C.H. Zhang, Z. Hua, G. Gao, S. Zhao, Y.D. Huang, Damping behavior and acoustic performance of polyurethane/lead zirconate titanate ceramic composites. Mater. Design. 46, 503-510 (2019).
4. S.S. Kim, S.B. Jo, K.I. Gueon, K.K. Choi, J.M. Kim, K.S. Churn, Complex permeability and permittivity and microwave absorption of ferrite-rubber composite at X-band frequencies. IEEE T. Magn. 27, 5462-5464 (2018).
5. C.Y. Lee, M.J. Leamy, J.H. Nadler, Frequency band structure and absorption predictions for multi-periodic acoustic composites, J. Sound Vib. 329, 1809-1822 (2018).
6. R. Rodriguez, E. Arteaga, D. Rangel, R. Salazar, S. Vargas, M. Estevez, Mechanical, chemical and acoustic properties of new hybrid ceramic-polymer varnishes for musical instruments, J. Non-Cryst. Solids 355, 132-140 (2019).
7. Y. Yohachi, J. John, H. Yasuharu, I. Kazuhiro, Effects of ceramic nanopowder dopants on acoustic attenuation properties of silicone rubber lens for medical echo probe, Jpn. J. Appl. Phys. 46, 4784-4789(2015).
8. H. Mei, Y.Y. Sun, L.D. Zhang, H.Q. Wang, L.F. Cheng, Acoustic emission characterization of fracture toughness for fiber reinforced ceramic matrix composites. Mat. Sci Eng. A-Struct: A 56, 372-376 (2017).
9. A. Bele, M. Cazacu, G. Stiubianu, S. Vlad, M. Ignat, Polydimethylsiloxane-barium titanate composites: preparation and evaluation of the morphology, moisture, thermal, mechanical and dielectric behavior, Compos. Part B 68, 237-245(2015).
10. B.C. Luo, X.H. Wang, Q.C. Zhao, L.T. Li, Synthesis, characterization and dielectric properties of surface functionalized ferroelectric ceramic/epoxy resin composites with high dielectric permittivity, Compos. Sci. Technol. 112, 1-7 (2015).
11. X. Liu, W.Y. Kuang, B.C. Guo, Preparation of rubber/graphene oxide composites with in-situ interfacial design, Polym. 56, 553-562 (2015).
12. C.H. Zhang, Z. Hu, G. Gao, S. Zhao, Y. D. Huang, Damping behavior and acoustic performance of polyurethane/lead zirconate titanate ceramic composites, Mater. Design 46, 503-510 (2019).
13. C. Zhang, J.F. Sheng, C.A. Ma, M. Sumita, Electrical and damping behaviors of CPE/$BaTiO_3$/VGCF composites, Mater. Lett. 59, 648-3651(2015).
14. J. Cai, Y.H. Li, W.M. Cai, Study on acoustic absorption mechanism of piezoelectric and electrical conductive polymeric composite PZT/CB/PVC, J. Biomat. Sci-Polyme. 23, 215-218 (2017).

15. H.H. Law, P.L. Rossiter, L.L. Koss, G.P. Simon, Mechanisms in damping of mechanical vibration by piezoelectric ceramic-polymer composite materials, J. Mater. Sci. 30, 2648-2655(2015).
16. N.N. Najib, Z.M. Ariff, A.A. Bakar, C.S. Sipaut, Correlation between the acoustic and dynamic mechanical properties of natural rubber foam: effect of foaming temperature. Mater. Design 32, 505-511 (2011).
17. S. Horiuchi, Y. Tokunaga, G. Giovannetti, S. Picozzi, H. Itoh, R. Shimano, R. Kumai, Y.Tokura, Above-room-temperature Ferroelectricity in a Single-component Molecular Crystal. Nature 436, 789-792 (2020).
18. R. Ginés, R. Libanori, A.R. Studart, A. Bergamini, M. Motavalli, P. Ermanni, Ceramic–polymer composites with improved dielectric and tribological properties for semi-active damping, Compos. Part B-eng. 72, 80-86(2015).
19. G. Gaunaurd H. Uberall, Resonance theory of the effective properties of perfornate solids, J. Acoust. Soc. 71, 282-295 (2018).
20. L.G. Yu, Z.H. Li, L.L. Ma, Theoretical analysis of underwater sound absorption of 0-3 type piezoelectric composite coatings, Acta. Phys. Sin-Ched. 61, 240-301 (2018).

Tables

Table 1 Basic proportion of NCB/BWZT/RTV composites

The mass ration of BWZT to RTV				2:3			
Contents of NCB (wt.%)		0	1	2	4	6	8

Table 2 d_{33} of NCB/BWZT/RTV composites with different NCB contents before and after polarization

wt.% of NCB		0	1	2	4	6	8
d_{33} (pC/N)	Before poling	58	62	64	65	68	68
	After poling	66	69	72	77	81	81

(For BWZT itself: d_{33} =546pC/N)

Figures

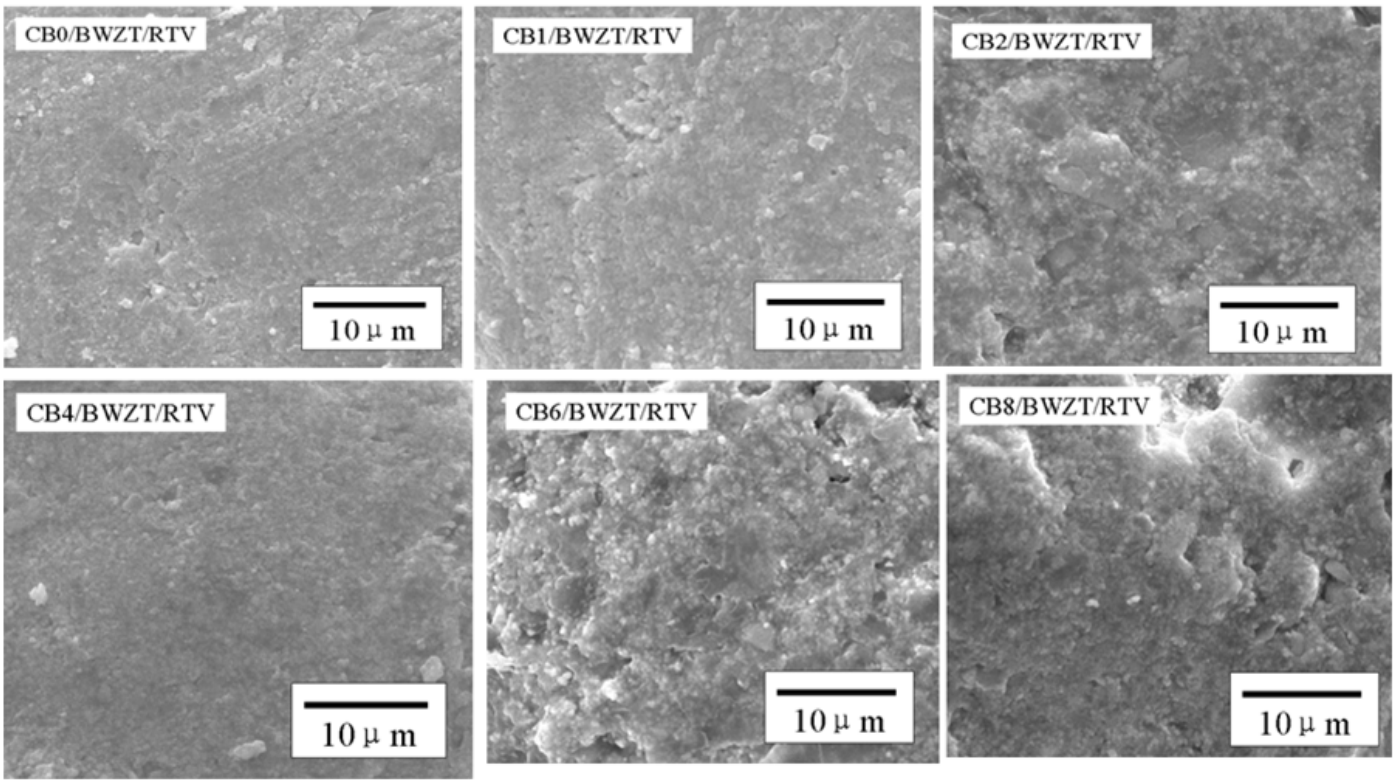

Figure 1

Morphologies of BWZT/RTV complex matrix and NCB/BWZT/RTV composites with different NCB amounts

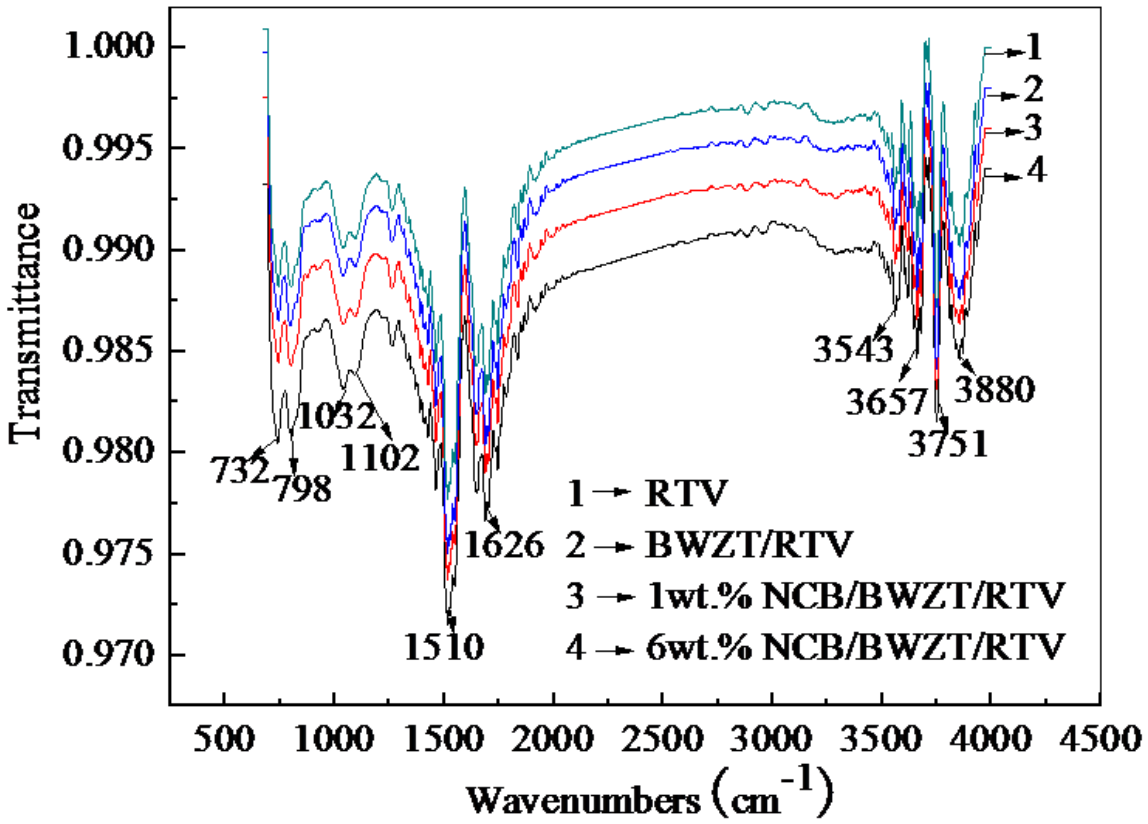

Figure 2

IR of RTV, BWZT/RTV complex matrix and NCB/BWZT/RTV composites with different NCB amounts

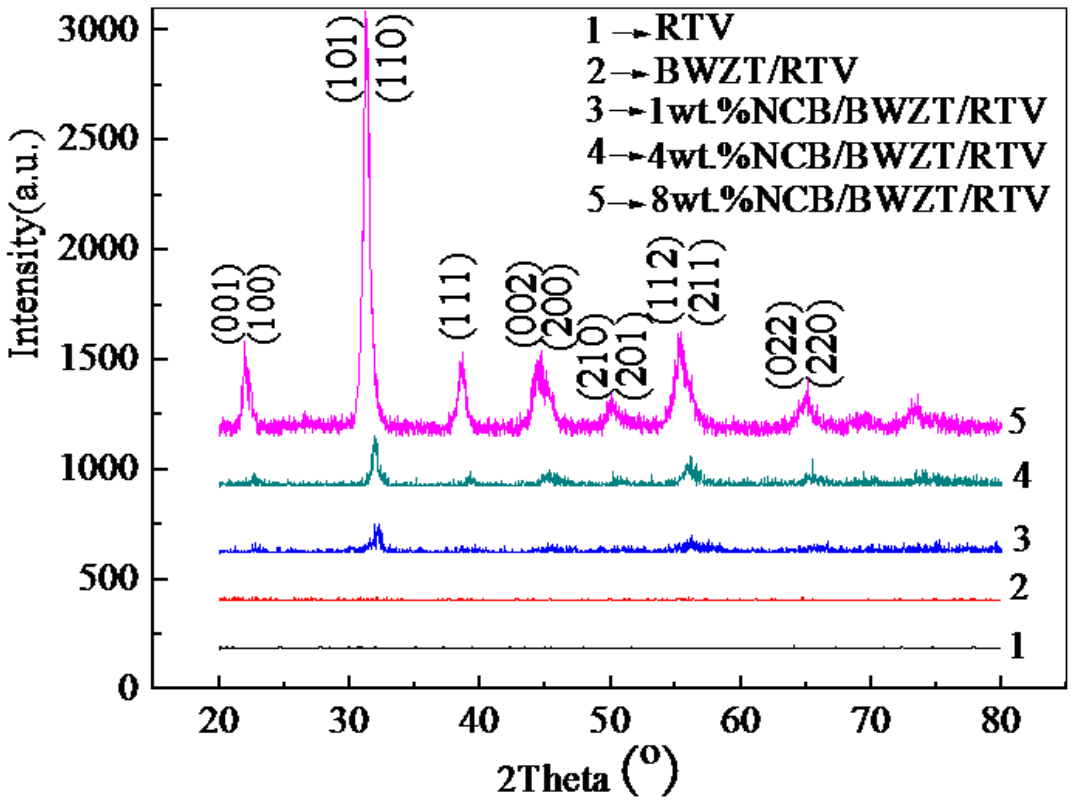

Figure 3

XRD of RTV, BWZT/RTV complex matrix and NCB/BWZT/RTV composites with different NCB amounts

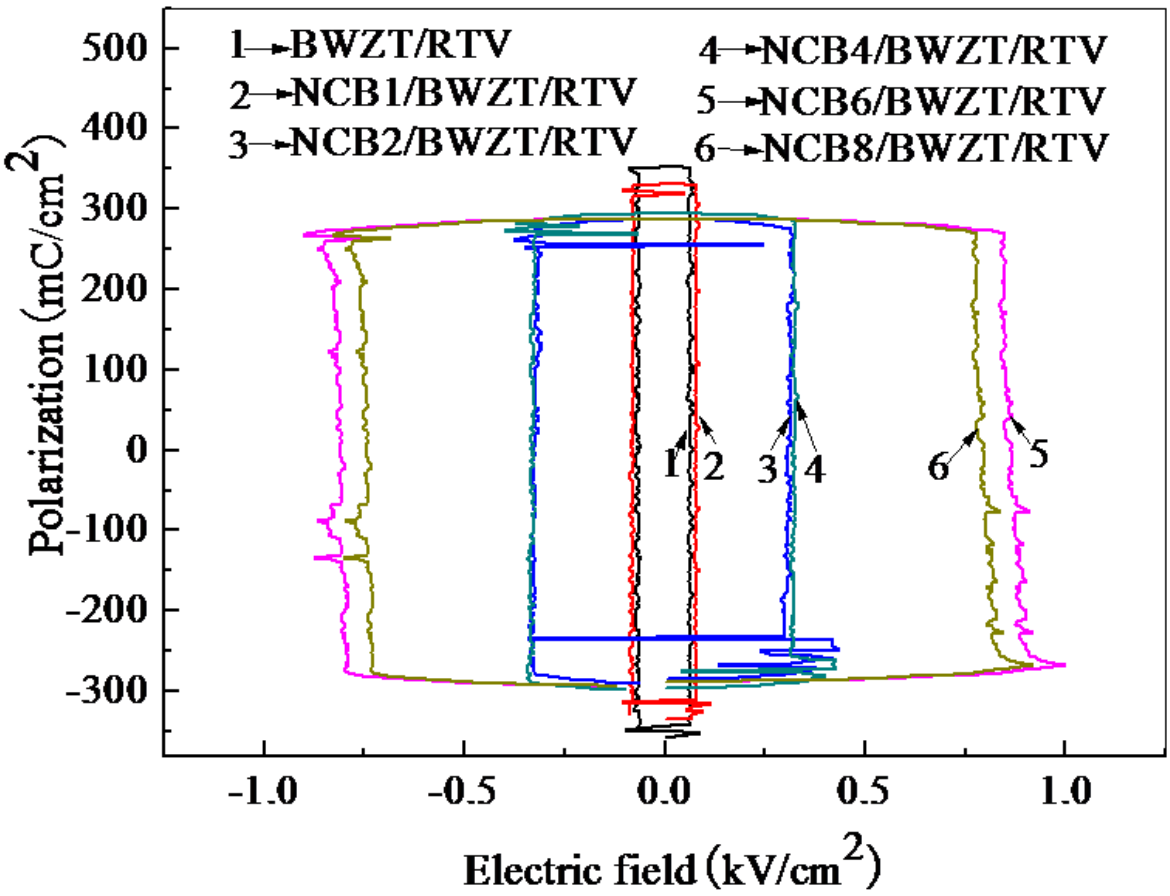

Figure 4

Ferroelectric hysteresis loops of BWZT/RTV complex matrix and NCB/BWZT/RTV composites with different NCB amounts

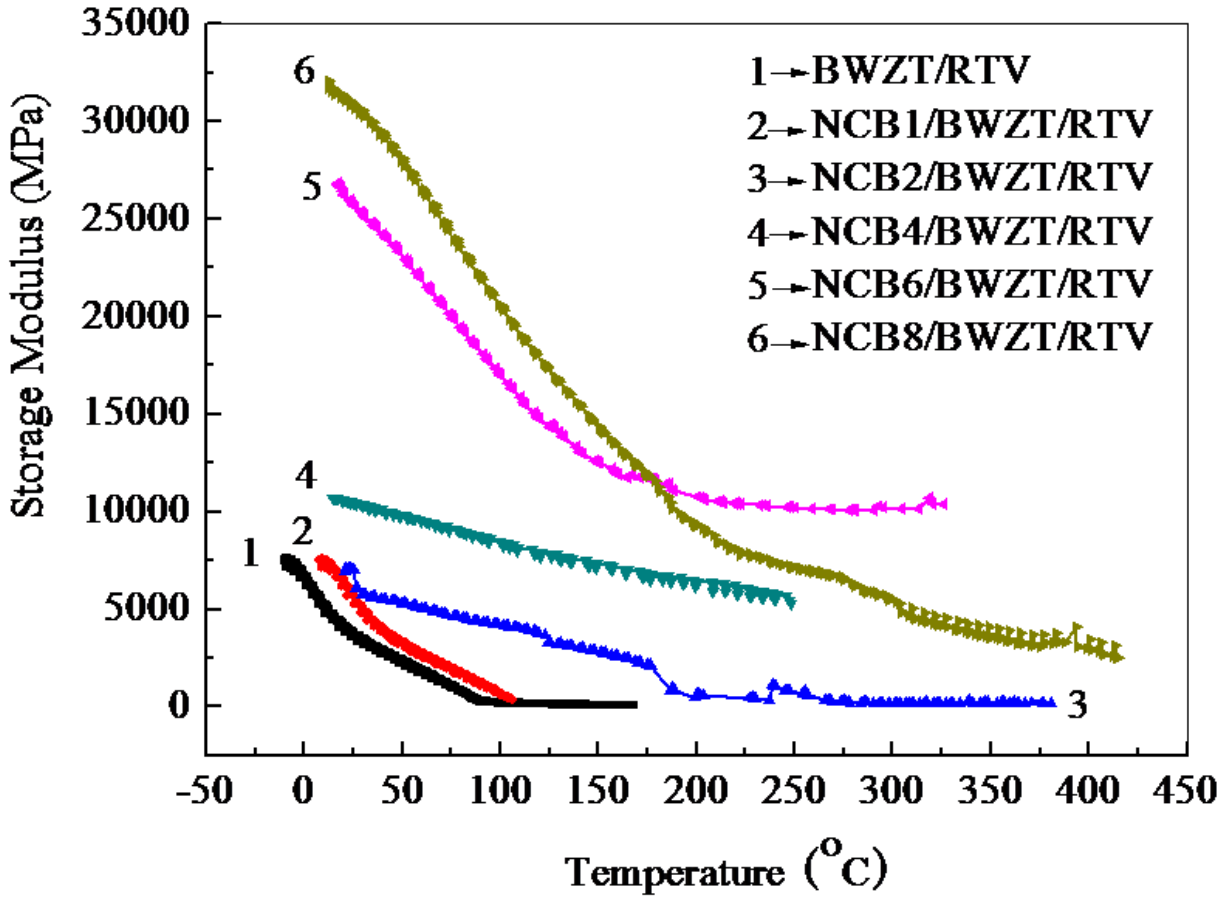

Figure 5

Storage modulus of BWZT/RTV complex matrix and NCB/BWZT/RTV composites with different NCB amounts

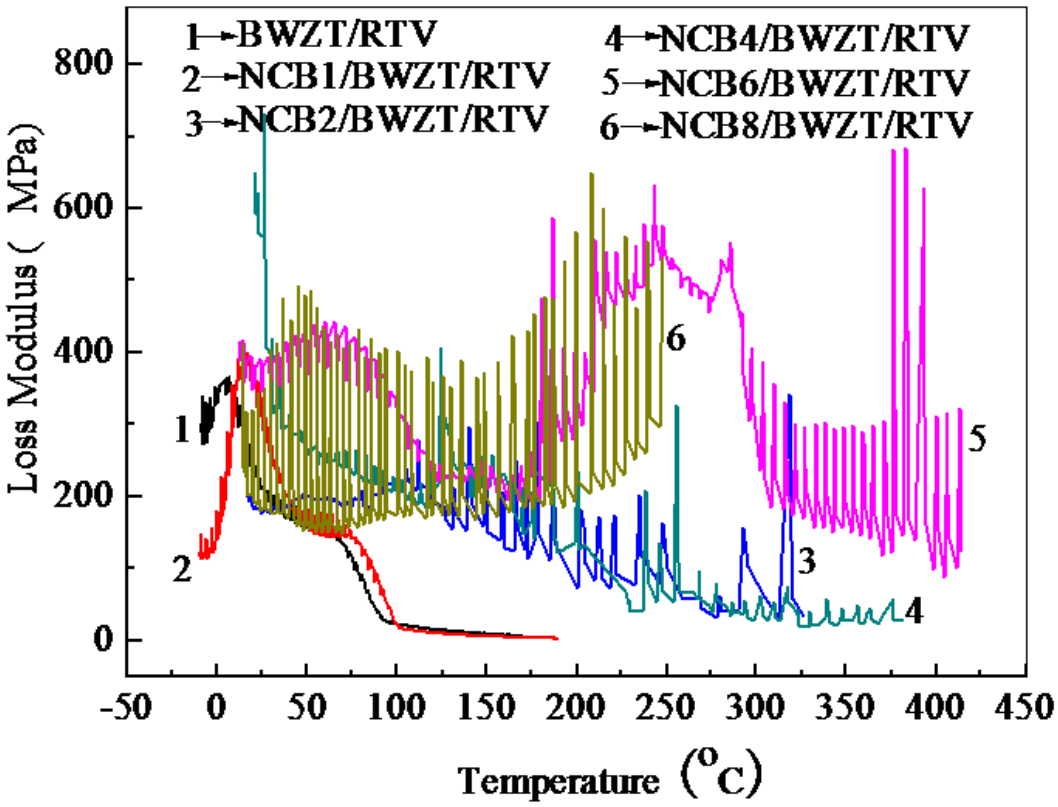

Figure 6

Loss modulus of BWZT/RTV complex matrix and NCB/BWZT/RTV composites with different NCB amounts

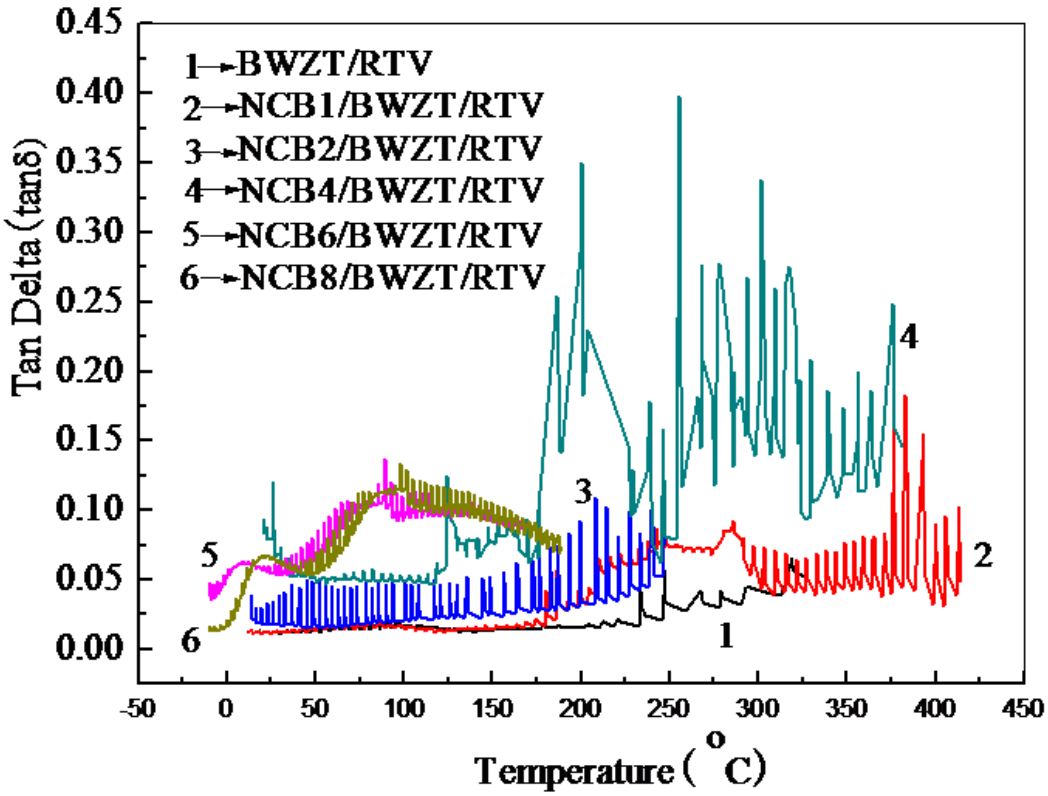

Figure 7

Dynamic mechanical properties of BWZT/RTV complex matrix and NCB/BWZT/RTV composites with different NCB amounts

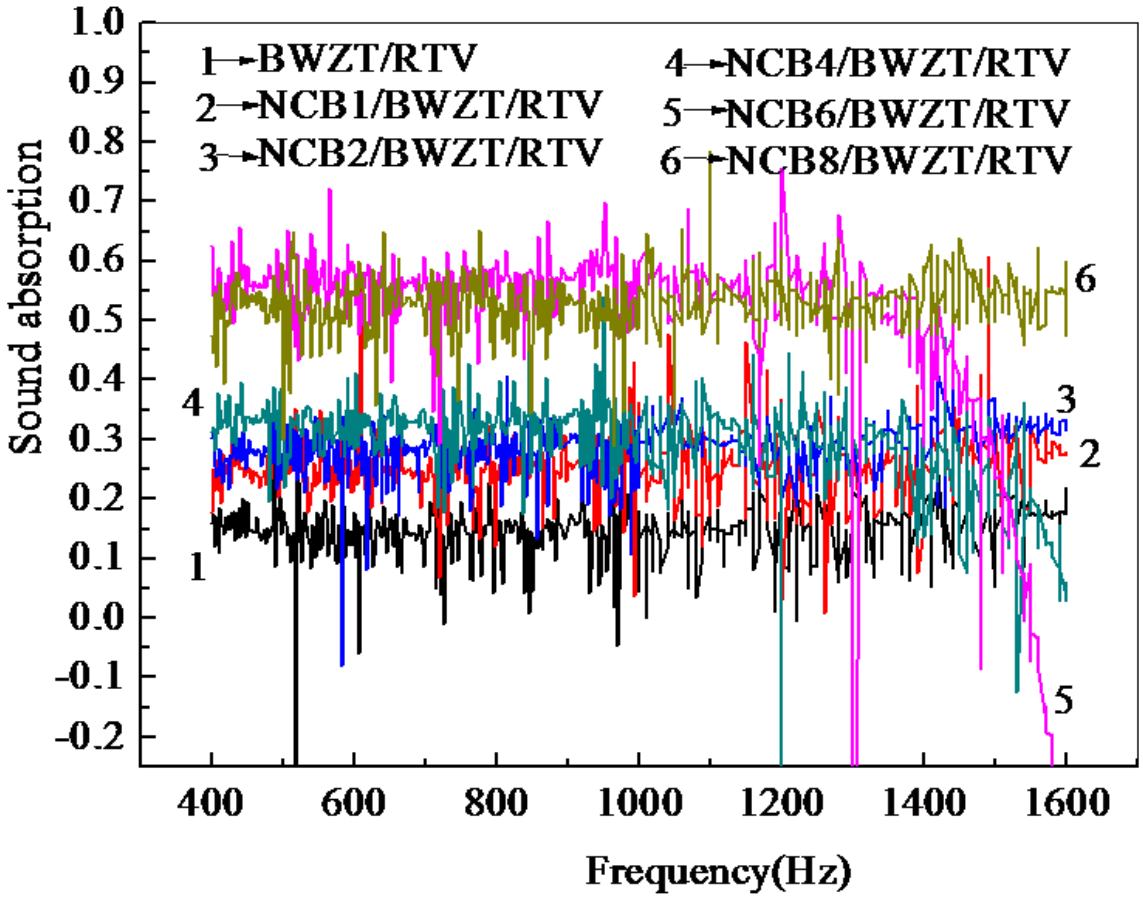

Figure 8

Sound absorption performances of BWZT/RTV complex matrix and NCB/BWZT/RTV composite with different NCB amounts

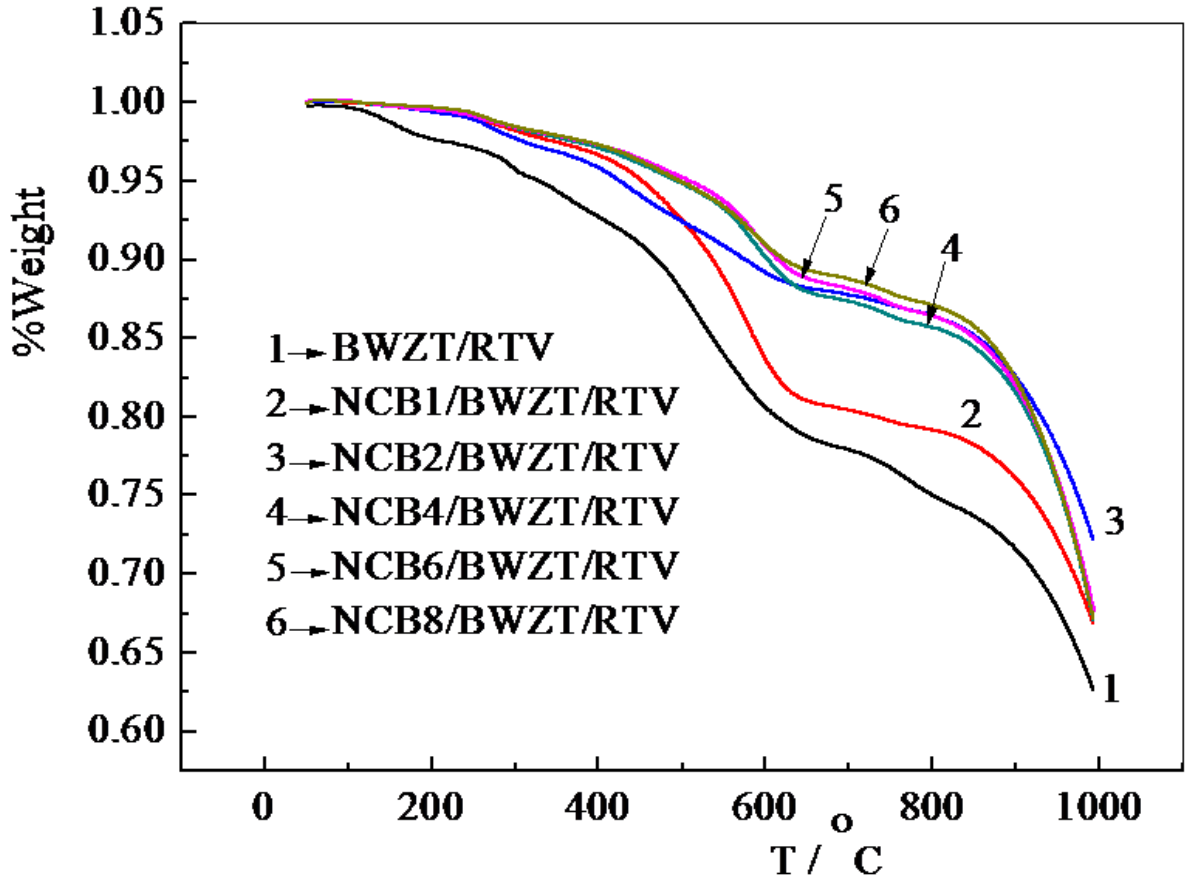

Figure 9

TG of BWZT/RTV complex matrix and NCB/BWZT/RTV composites with different NCB amounts